NRC·CNRC CNRC·NRC
Institute for Research in Construction
Institut de recherche en construction
http://www.nrc-cnrc.gc.ca/irc

Impact of air intrusion on the wind uplift performance of fully bonded roofing assemblies

NRCC-49721

Baskaran, B.A.; Molleti, S.; Sexton, M.

February 2009

A version of this document is published in / Une version de ce document se trouve dans:
Construction and Building Materials, 23, (2), pp. 889-901, DOI:
10.1016/j.conbuildmat.2008.04.010

National Research Council Canada Conseil national de recherches Canada
Canada

Impact of Air Intrusion on the Wind Uplift Performance of Fully Bonded Roofing Assemblies

A. Baskaran[1], S. Molleti[2] and M. Sexton[3]

National Research Council Canada
1200 Montreal Road
Ottawa, ON K1A OR6
Canada

ABSTRACT

Wind performance investigation is critical in the design of durable roofing assemblies. In North America, mainly two types of low slope roofs, conventional and inverted, are in practice depending on the placement of the membrane in the assembly. As part of the conventional low-sloped roofs, in a Fully Bonded Assembly (FBA) the insulation is mechanically attached and waterproof membrane is bonded to the insulation using adhesives. Recent field investigations of roof failures after major hurricanes indicated that FBA are susceptible to high wind events. To understand the response of the FBA under dynamic environment, an extensive experimental study has been carried out by the SIGDERS – *Special Interest Group for Dynamic Evaluation of Roofing Systems*, at the National Research Council. The present study focuses on the impact of air intrusion on wind uplift performance of these assemblies. Airflow control is usually achieved by including a barrier/retarder in the roofing assembly. Assembly with barrier improved the wind uplift rating by two fold when compared to an assembly without barrier. Use of staggered insulation arrangement can provide similar air retarding effect as a barrier and can therefore sustain similar wind uplift pressures compared to an assembly with barrier.

Key words
Wind, Roof, Air intrusion, Uplift, Fastener, Load, Dynamic Test, Failure mode, Adhesive, Staggered arrangement

1. *Group Leader, Corresponding Author, Tel: +613-990 3616; Fax: 613-998-6802;bas.baskaran@nrc.ca*
2. *Research Officer*
3. *Former Technical Officer*

1. Introduction

In North America, two main types of low slope roofs are in practice depending on the placement of the membrane in the assembly (Baskaran, et al 1997):

> *Conventional roofing assembly*: The membrane is at the top of the insulation and is directly exposed to environmental elements. The conventional roofs may be either the Single-ply roofing system (SPR) or a Built up roofing system (BUR).
>
> *Inverted roofing assembly:* It is also known as protected roofing assembly. The membrane is placed below the insulation and, thus is protected from environmental elements such as wind, rain, UV and temperature.

Within the conventional single ply roofing assembly three different types exist as follows:

> Mechanically attached SPR: The membrane is attached to the structural substrate either along strips or at discrete points using fasteners. The attachments consist of the mechanical fasteners and plates or metal or polymer batten.
>
> Fully Bonded SPR: The membrane is adhered to the insulation by solvent or water-based adhesive or hot bitumen and the insulation is mechanically attached to the structural deck.
>
> Loose Laid SPR (ballasted configuration): The single-ply membrane is loose laid and held down by the weight of concrete pavers. However, at the building perimeters, the membrane is attached with the roof/wall junctions.

The present study focuses on the wind uplift performance of fully bonded single ply roofing assembly. The fully bonded single-ply roofing assembly (here after abbreviated as FBA) comprises of the components: deck, barrier, insulation, fastener plate, fastener, adhesive and membrane. Wind-uplift resistance of FBA depends on several factors namely, on the application and bonding strength of the adhesive, bonding strength of the membrane with insulation and fastener plates, fastener density of the insulation board, insulation thickness, and curing time of the assembly.

Wind uplift resistance of FBA is different from that of MAS (Baskaran and Smith, 2005). Figure 1 illustrates the wind effects on FBA. As shown in the figure, the entire roofing assembly acts as single unit though each component of the roofing assembly offers certain resistance to the wind uplift force. This can be illustrated through a force-resistance link diagram. All resistance links should remain connected for the assembly to be durable and to keep the roof properly in place.

Figure 1. Wind Uplift Resistance of FBA

Existing studies in the literature focused on the wind uplift resistance evaluation of MAS with different membranes - Assemblies with PVC membranes (Baskaran and Lei, 1997), Assemblies with modified bituminous membranes (Chen and Baskaran, 1998) and Assemblies with TPO membranes (Baskaran, Lei and Richardson, 1999). However, no studies exist in the literature documenting the performance of FBA. Recent field investigations of roof failures after major hurricanes indicated that these assemblies are equally susceptible to high wind events (NRCA, 2004 and RICOWI, 2006). Recent standard developed by the Single Ply Roofing Institute (SPRI, 2005) address only the bonding strength of insulation to the steel deck on small-scale specimens.

To understand the response of the FBA under dynamic environment, an extensive experimental study has been carried out by the SIGDERS – *Special Interest Group for Dynamic Evaluation of Roofing Systems* - at the National Research Council Dynamic Roofing Facility (Baskaran and Sexton, 2002). Recently, wind uplift performance of FBA was reported by Baskaran et al (2006 a) by investigating the effect of three parameters on wind uplift, namely, curing period, fastener plate configuration and insulation thickness. This paper contributes by presenting the impact of air intrusion on the wind uplift performance of FBA. To limit air intrusion, new mockups were constructed with barriers (retardres) and experiments were completed for wind uplift rating. Measured responses were compared side by side for assemblies with barrier to assemblies without barrier. From this investigation, a novel approach for the insulation arrangement was developed and concluded that assemblies with staggered arrangement can have equal wind uplift resistance as that of assemblies with barrier.

2. Experimental Approach

Experimental work was carried out at the Dynamic Roofing Facility (DRF) established at the Institute for Research in Construction at the National Research Council of Canada (IRC/NRC). DRF consists of a bottom frame of adjustable height upon which the roof specimen and a removable top chamber are installed (Figure 2). The design allows for the installation and study of roof assemblies of different thicknesses up to 500 mm (18") as well as the evaluation of sloped roofs. The bottom frame and top chamber are 6100 mm (240") long and 2200 mm (86") wide and 800 mm (32") high. The top chamber is equipped with six windows for viewing, and with a gust simulator, which consists of a flap valve connected to a stepping motor through a timing belt arrangement. Pressure suction as high as 10 kPa (209 psf) over the roof assembly is produced by a 37 KW (50HP) fan with a flow rate of 2500 L/sec (5300 cfm). A computer, using feedback signals, controls the operation of the DRF. The computer regulates the fan speed in order to maintain the required pressure level in the chamber. Operation of the flap valve simulates the gusts in the form of uniform cyclic pressure loading over the surface of the roofing system. Closing the flap valve allows pressure to build in the chamber, while opening the valve bleeds the pressure. Also, the test facility has instrumentation for measuring the dynamic response for the specimen. More information of the DRF features is given in Baskaran and Lei (1997).

Figure 2. FBA on the Dynamic Roofing Facility

All assemblies were subjected to the simulated wind dynamics in accordance to CSA A 123.21-04 standard's load cycle. The CSA A 123.21-04 load cycle (CSA, 2004) was developed based on the wind-tunnel studies of full-scale roof assemblies. Studies were made of 3048 × 3048 mm (120" × 120") roof assemblies using the National Research Council's (NRC's) 9000 × 9000 mm (360" × 360") wind tunnel. Two series of investigations were carried out using two distinct roofing membranes. The first series dealt with a reinforced Poly Vinyl Chloride (PVC) membrane and the other with a non-reinforced Ethylene Propylene Diene Monomore (EPDM) membrane. Different configurations were tested for variation in building heights, wind speed and wind direction. The obtained unsteady histories of wind pressures were used for the load cycle development. The details of the developed load cycle can be found in a report by Baskaran et. al (1999).

Figure 3 shows SIGDERS load cycle and it has five rating levels (A to E). The test pressure on the Y-axis corresponds to the design pressure, in accordance with local building codes or wind standards. A summary of the load cycle follows:

- As shown in Figure 3, the SIGDERS dynamic protocol has five rating levels (A to E). To evaluate a roof assembly for a specific wind resistance, all the gusts corresponding to Level A should be applied.
- Each level consists of eight load sequences with different pressure ranges, depicted in Figure 3. The eight load sequences can be divided into two groups. Group 1 represents wind-induced suction over a roof assembly. It consists of four sequences, where the pressure level alternates between zero and a fixed pressure. Group 2 represents the effects of exterior wind fluctuations combined with a constant interior pressure on a building. Internal pressure variations are explicitly codified in the recent North American wind standards (ASCE 7-2005, NBCC 2005). The SIGDERS test protocol accounts for such variations.
- The test pressure ratios (y-axis) for a test can be calculated from the design pressure, in accordance with local building codes or wind standards. The pressures for each load sequence are calculated as percentages of the test pressure.
- To evaluate the ultimate strength of the roofing assembly, testing should be started at Level A and should be continued when moving from one level to another. To obtain a rating, all specified numbers of gusts in each level must be completed without any resistance link failure. As discussed in the Figure 1, the assembly is considered as "Failed", even if one resistance link fails.

Figure 3. SIGDERS Dynamic Load Cycle

3. Mockup Construction Process

Five assemblies (Table 1) were constructed having size 2000 mm (79") wide and 3048 mm (120") length (Figure 4). The construction procedure can be described in five steps as shown in Figure 5:

Table 1. Mock-ups Details and Nomenclature

Figure 4. Typical Layout of FBA with Barrier

Deck Installation: Two deck pieces cut at length of 3048 mm (120") and width of 1000 mm (39") were overlapped and fastened with two 150 mm x 150 mm (6" x 6") wooden beams spaced at 1830 mm (72") o/c using 12 mm (½") carriage bolts and 76 mm (3") wood fasteners.

Barrier Installation: Gypsum support boards of 1219 mm x 2438 mm x 13 mm (48'" x 96" x 0.5") were loose laid on the steel deck. As the test assembly spanned 3048 mm (120") in length and 2000 mm (79") in width, the gypsum support boards were laid with the longer dimension parallel to the width of the assembly, thereby accommodating two full boards 1219 mm x 2006 mm (48"x 79") and one half board of 610 mm x 200 mm (24" x 79"). A continuous layer of 6 mil (0.006 in.) thick polyethylene sheet was then loose laid over the gypsum support boards, ensuring an adequate overhang along the sides of the assembly.

Figure 5. Mock-up Construction Process of FBA with Barrier

Insulation Installation: Two full insulation boards of 1219 mm x 2006 mm x 50 mm (48" x 79" x 2") and two partial boards of 305 mm x 2006 mm x 50 mm (12" x 79" x 2") were installed on the steel deck. The full boards are installed in the middle with the long edges perpendicular to the steel deck flutes and the partial boards are installed on the sides as shown in Figure 11. A2 and A3 had staggered two layers of 50 mm (2") thick insulation boards in arrangement. The boards were fastened using # 15 - 127 mm (5") long fasteners and 73 mm (2⅞") diameter hexagonal metal plate. For A1, A2 and A3 each insulation board had a fastener density of one fastener per 0.17 m^2 (1.8 ft^2). Fastener density of A4 was 0.24 m^2 (2.6 ft^2), and in the case of A5 the fastener density was 0.5 m^2 (5.3 ft^2)

Membrane Installation: Two sheets of 1830 mm (72") wide 45 mil TPO membrane were hot air welded together to form a continuous waterproofing layer. The membrane was then laid out squarely over the insulation boards along the width of the assembly, and clamped at one end, ensuring minimum overhang of 203 mm (8") of membrane along the width of the assembly. The membrane is then folded in half, so as to expose both the membrane underside and the insulation facer surface. Each surface was then swept and cleaned. (Figure 5)

Adhesive Application: The adhesive was applied on both the membrane bottom surface and insulation top surface at a quantity of 1 Gal/70 ft^2, using conventional paint rollers and sleeves. The surfaces were then left to cure for a period of approximately 30 minutes or until the surface is "tacky" to touch. At that point the membrane side is flipped and allowed to adhere to insulation surface using a spreading applicator as shown in Figure 5. All measures were taken to ensure that there was no air trapped under the membrane. The same procedure is repeated for the other half of the membrane.

The above-mentioned systematic approach was followed for all assembly constructions as specified by the material manufacturer according to the amount of adhesive used per mock-up, the amount of curing time prior to application, and the membrane seaming weld parameters. Further, all assemblies were constructed by the same roof applicator in order to minimize any errors resulting from differences in construction techniques and all assemblies were stored undisturbed under same ambient conditions. Component details of an assembly, labeled as ***Aref***, are also included in the Table 1. Data from ***Aref*** is taken from Baskaran et al (2006) as a reference assembly with out barrier to compare with the present investigations.

4. Results and Discussion

This section presents the measured responses in three sections as follows:

1) Impact of air intrusion on the wind uplift resistance
2) Side by side comparison of the wind uplift resistance of assemblies with new insulation layers arrangement to assemblies with barrier.
3) Effect of fastener density in the wind uplift resistance.

Figure 6 compares the measured response of ***A1*** (with barrier) to ***Aref*** (without barrier). ***A1*** sustained a maximum pressure of 5.5 kPa (115 psf) with fastener load of 1.3 kN (295 lbf) and passed all sequences up to Level B of the CSA A123.21-04 dynamic test protocol. When the applied pressure was 6.5 kPa (135 psf), the assembly failed at the loading sequence 4, gust number 25 of Level C. Comparing with the ***Aref*** data, it is clear that there is two fold improvement in the wind uplift resistance. This improvement can be mainly attributed to the inclusion of barrier and it impact in limiting air intrusion in to the assembly.

Figure 6. Comparison of the Response Plots of FBA with Barrier (A1) and without Barrier (Aref)

This can be clearly demonstrated by comparing the failure modes of these two assemblies as shown in Figure 7. A key message is, in ***Aref*** air intrusion through the joints of steel deck and insulation was acting as a catalyst for the failure propagation of the insulation facer delamination. Note that that this assembly failed to have a barrier that can minimize air intrusion at the deck level. When it is subjected to suction at the membrane level, the bonding strength of the adhesive interface between the membrane and insulation causes the lifting of the insulation boards, which is resisted by the insulation fastener attachment. To equalize the suction pressures, the inside air will tend to move upward into the assembly. In the absence of a barrier, this air movement through the joints has a tendency to weaken the adhesive interface between the insulation and membrane, propagating delamination failure of membrane or insulation facer. ***A1*** failed due to structural foam failure of the insulations. In ***A1,*** the presence of barrier restricts the air intrusion into the assembly and reduces the stress (failure propagation) at the adhesive interface between the membrane and insulation. Due to this response, the load from the adhesive layer is transferred to the insulation. When the pressure is 5.5 kPa (115 psf), the wind-induced load at the fastener was 1.3 kN (295 lbf). High pressure might have induced loads in excess of the compressive strength [0.172 N/ mm^2 (25 psi)] of the insulation board and ultimately leading to the cracking of the insulation foam. This will be further discussed under Figure 15.

Figure 7. Comparison of the Failure modes of FBA with Barrier (A1) and without Barrier (Aref)

Depending on thermal requirements of a building envelope, in a roofing assembly the insulation thickness can vary. Mostly in practice, the total thickness can be achieved by having multiple layers of insulation. The present study identified a new staggered insulation arrangement such that it can control air intrusion into the assembly in additional to the thermal requirement. By doing so, the present study attempts to answer whether the staggered arrangement can be as effective as that of having a barrier in an assembly. Figure 8 illustrates the cross-sectional view of an assembly with staggered arrangement of two layers 50 mm (2") thick insulation boards without barrier (labeled as ***A2***). Apart from the varying insulation thickness the remaining components and arrangements {curing time (28 days), fastener density [0.17 m^2 (1.8 ft^2)/ fastener]} were similar to ***A1***.

Figure 8 also shows the measured pressure and load time histories obtained from ***A2***. ***A2*** sustained a maximum pressure of 5 kPa (105 psf) and failed during the wind gusts of 5.7 kPa (120 psf). The corresponding induced sustained fastener load was 1.1 kN (252 lbf), indicating that the wind uplift performance of ***A2*** was similar to ***A1***. This can be mainly attributed to the air intrusion control into the assembly. ***A1*** had a barrier to control the air movement, while in ***A2*** the staggered insulation boards provided the necessary air retarding effect. With the staggered arrangement of insulation boards, air entering through the joints of steel deck into the bottom insulation layer is partially retarded by the top insulation layer from moving into the adhesive interface. With the air intrusion restricted, the adhesive strength between the membrane and insulation is not affected, thus transferring the uplift pressure to the insulation.

Figure 8. Response of A2 with Staggered Insulation Arrangement – Pressure & Load

After the wind uplift test, ***A2*** was examined for its failure modes (Figure 9). ***A2*** failure mode was combination of ***Aref*** and ***A1***. Similar to ***Aref***, facer delamination was observed and foam structure failure was observed same as ***A1***. Since, there is no barrier in ***A2*** (same as ***Aref***) partial air intrusion caused the facer delamination and on the other hand due to staggered arrangement, air intrusion is controlled better than ***Aref*** causing foam failure. Closer examination of ***A2*** indicated foam cracking only at the top insulation layer, while the bottom insulation layer had no signs of damage. Note that there is no adhesive interface between the two layers.

Figure 9. Failure Mode of A2 with Staggered Insulation Arrangement without Barrier

Due to the mixed failure mode of ***A2***, it has been decided to examine an assembly similar to ***A2*** by introducing the barrier. Figure 10(a) shows the cross section of such assembly, ***A3***, with staggered insulation arrangement and barrier. All other parameters are kept constant. During the wind test, ***A3*** was able to resist an uplift pressure of 6.5 kPa (135 psf), however, it could not sustain all the sequences of the Level C as illustrated in Figure 10(b). According to the CSA A123.01-04 Standard, ***A3*** can be rated to a sustained pressure of 5.5 kPa (115 psf) with a fastener load of 1.3 kN (301 lbf).

Figure 10(a). Cross Sectional View of A3 - Staggered Insulation Arrangement with Barrier

Figure 10(b). A3 Pressure and Load Response

Figure 11 shows the observed failure mode of ***A3***. It had the similar failure mode as ***A2*** with top layer undergoing foam failure and the bottom layer being devoid of any kind of damage. However, in ***A3*** it was observed that the cracking of the insulation foam was more severe compared to ***A1*** and ***A2,*** also the top insulation layer shows a cone foam failure around the fastener plate. This type of cone failure was not observed either in ***A1*** or ***A2***. This failure pattern led to the conclusion that with the barrier and staggered insulation arrangement together controlled the air intrusion better than other assemblies, which allowed the assembly to resist a higher uplift pressure of 6.5 kPa (135 psf) compared to 5 kPa (105 psf). Due to this air intrusion control, the bonding strength of the adhesive interface between the membrane and insulation was not weakened, thereby transferring the uplift load from the adhesive interface to the insulations. At high pressures, the composite behavior of membrane and insulation foam might have led to high deformations of the top layer leading to the cone failure around the fastener plate.

Figure 11. Failure Mode of the A3

Figure 12 summarizes the relative wind uplift performance of:

Aref [a layer of insulation - without barrier] with
A1 [a layer of insulation - with barrier],
A2 [staggered insulation arrangement - without barrier]
A3 [staggered insulation arrangement - with barrier]

Relative ratios were calculated as shown in Figure 12. Observations can be summarized as follows:

1. Controlling air intrusion improves the wind uplift rating to maximum of about two fold.
2. One can achieve similar wind uplift resistance (1.75 vs. 1.92) either by incorporating a barrier at the deck level or by arranging multilayered insulation in staggered fashion.
3. Only the top layer contributed to the wind uplift resistance in a multilayer arrangement due to the fact that there is no adhesive bonding among the layers.

Figure 12. Comparison of the Relative Wind Uplift Performance of FBAs

As discussed, the cone failure mode of the insulation foam indicates that the insulation board undergoes deformation during wind uplift with restrained around the fastener plates. Thus the deformation of the insulation board is mainly determined by the fastener density (number of fasteners per insulation board) and layout. The above-discussed assemblies had a fastener density of 0.17 m^2 (1.8 ft^2). In other words from the surrounding area of 0.17 m^2 (1.8 ft^2) each fastener transfers induced load to the deck. To further investigate the effect of fastener density, two new assemblies ***A4*** and ***A5*** were constructed with the reduction in fastener densities. ***A4*** had an insulation board fastener density of one fastener per 0.24 m^2 (2.6 ft^2) and ***A5*** had a fastener density of one fastener per 0.5 m^2 (5.3 ft^2) as shown in Figure 13. The wind uplift behaviour from these two assemblies was compared with ***A1***.

Figure 13. Fastener Density Variations

Figure 14 compares the sustained wind uplift pressures of the three assemblies. ***A1*** with a fastener density of one fastener per 0.17 m^2 (1.8 ft^2) sustained a wind uplift pressure of 5.6 kPa (115 psf). Decreasing the fastener density to 0.24 m^2 (2.6 ft^2) for ***A4***, the wind uplift rating reduced to 3.6 kPa (75 psf) [30% reduction compared to A1]. ***A5*** with further reduction of fastener density to 0.5 m^2 (5.3 ft^2) sustained only a wind uplift resistance of 1.4 kPa (30 psf).

Figure 14. Effect of Fastener Density on the Wind Uplift Rating of FBA with Barrier

All the three assemblies failed due to cracking of the insulation foam. Note that the measured load of the insulation fastener for all the three assemblies was in the neighborhood of 1.1 kN (250 lbf) and foam failure occurred above 1.3 kN (300 lbf). This can be attributed to the compressive strength of the insulation. During wind uplift, the upward deflection of the insulation is dependent on the insulation attachment with the deck as along as the adhesive interface between the membrane and insulation is intact. As discussed in the previous section, presence of barrier mitigated the effect of air intrusion into the assembly and thereby transferring the weakest link from the adhesive interface to the insulation attachment. Then the fastener density of the insulation attachment characterizes the deflection of the insulation board. ***A1*** with a fastener density of one fastener per 0.17 m^2 (1.8 ft^2) has minimum upward deformation compared to others. The wind-induced load at the fastener might have exceeded the reported compressive strength [0.172 N/ mm^2 (25 psi)] of the insulation ultimately leading to the cracking of the insulation foam. Reducing the fastener density to 0.24 m^2 (2.6 ft^2) in ***A4*** made the insulation susceptible to higher deformations, which elevated the stress on the insulation fasteners thereby subjecting the insulation to failure. Similar failure mode was observed in ***A5***, however, with server degree of insulation cracking. With less fasteners and increased adhesive contact area between the membrane and insulation, the insulation boards were subjected to high shear loads compared to ***A1*** and ***A4*** as shown in Figure 15. As the force required to resist these loads surpassed the compressive strength of the insulation board, the insulation underwent foam failure. The maximum measured fastener force for ***A5 was*** 1.08 kN (246 lbf) at a low-pressure of 1.4 kPa (30 psf) justifies the above fact. Based on the observed failure modes it can be concluded that the degree of cracking of the insulation board is inversely proportionate to the number of fasteners installed per board.

Figure 15. Deformation of the FBAs with Different Fastener Densities

5. Concluding Remarks

The present study emphasized the impact of air intrusion on wind uplift resistance of FBA. Air intrusion can have significant impact and it can significantly alter the wind uplift behaviour of the FBA. Based on the presented results and discussions, the following conclusions can be drawn:

- Wind uplift performance is improved on assemblies with barrier. An improvement of about 50% has been measured in the wind uplift rating for the tested assemblies with barrier. This improvement in wind uplift performance can be mainly attributed to the air retarding effect of the barrier, which lowers the stress on the adhesive bond and reduces the failure propagation at the adhesive interface.
- Using insulations in staggered arrangement can provide similar air retarding effect as a barrier and thus assemblies with that arrangement can sustain similar wind uplift pressures as that of an assembly with barrier.
- When insulations are mechanically attached to deck, the fastener density has a major role in the wind uplift resistance of the FBA. Assembly with higher fastener density can sustained higher wind uplift pressures compared to assemblies with lower fastener densities.

Roof can be divided into three zones namely field, edge and corner (ref Figure 1). Air leakage in the field zone of a roof might not be same as that of a corner. This is due to the fact that the corner zone has numerous junctions and terminations and also it may be subjected to higher wind pressures compared to the field zone. The present study evaluations are limited to the field zone. Also, the present study illustrated the importance of air leakage on wind uplift, however, as how much air intruded into the assembly is not presented in this paper. Readers interested in the quantification of the air leakage are referred to Baskaran, Molleti, Booth, (2006).

6. References

American Society of Civil Engineering (2005), Minimum Design Loads for Building and Other Structures, SEI/ASCE 7-04, New York, USA 10017-2398.

Baskaran, A., Paroli R. M. and Booth R. J. (1997), “Wind performance evaluation procedures for roofing systems current status and future trends,” Fifth International Conference on Building Envelope Systems and Technology, BATH, U.K., pp. 37-52.

Baskaran, A. and Lei, W. (1997), "A New Facility for Dynamic Wind Performance Evaluation of Roofing Systems", *Proceedings of the Fourth International Symposium on Roofing Technology*, NRCA/NIST, Washington, D.C., U.S.A., pp. 168 -179.

Baskaran, A., Lei, W. and Richardson C. (1999), “Dynamic Evaluation of Thermoplastic Roofing Systems for Wind Performance,” *Journal of Architectural Engineering*, ASCE, vol. 5, No 5, pp. 16-24.

Baskaran, A., Chen Y. and Vilaipornsawai U. (1999), “A new dynamic wind load cycle to evaluate flexible membrane roofs,” Journal of Testing & Evaluation, 27, (4), July, pp. 249-265.

Baskaran A., Ladubec, C., Sexton, M. (2002), “SIGDERS Wind Uplift Resistance Data on Fully Bonded Single Ply Roofing Systems – Effect of Vapor / Air/ Barrier”, *Research Report, Institute for Research in Construction, National Research Council Canada,* IRC -RR # 115.

Baskaran, A., Smith, T.L., (2005), “A Guide for the Wind Design of Mechanically Attached Flexible Membrane Roofs” National Research Council Canada, Ottawa, Ontario, Canada, K1A 0R6

Baskaran, A., Molleti, S., Sexton, M., (2006 a), " Wind Performance Evaluation of Fully Bonded Roofing Assemblies,” Submitted *to the Journal of Construction and Building Materials.*

Baskaran, A., Molleti, S., Booth, R.J, (2006), " Understanding air barriers in mechanically attached low slope roofing assemblies for wind uplift," *Paper accepted to the 3rd International Building Physics/Science Conference, August 27th –31st. Montreal, Canada*

Chen .Y., Baskaran, A., Lei, W. (1998), "Wind load resistance of modified bituminous roofing systems," *Construction and Building Materials,* 12, (8), December, pp. 471-480.

CSA Number A123.21-04 (2004),”Standard test method for the dynamic wind uplift resistance of mechanically attached membrane-roofing systems, Canadian Standards Association, Canada.

National Roofing Contractors Association (2004), “Hurricane Charley: A Preliminary Report”, *Professional Roofing Magazine*, NRCA, October.

National Research Council Canada (2005), National Building Code of Canada, Ottawa, Ontario, Canada, K1A 0R6.

SPRI (2005), “ Standard Field Test Procedure for Determining The Mechanical Uplift Resistance of Insulation Adhesives over Various Substrates”, ANSI/SPRI IA-1 2005.

RICOWI, Inc. (2006), “ Hurricanes Charley and Ivan Wind Investigation Report”. Roofing Committee on Weather Issues Inc., McDonough, Georgia, March, pp 286

7. Acknowledgements

The presented research is being carried out for a consortium - Special Interest Group for Dynamic Evaluation of Roofing Systems (SIGDERS). SIGDERS was

formed from a group of partners who were interested in roofing design. These partners included:

Manufacturers	Atlas Roofing Corporation, Canadian General Tower Ltd., Carlisle Syn Tec., GAF Materials Corporation, GenFlex Roofing Systems, Firestone Building Products Co., IKO Industries Ltd., ITW Buildex, Johns Manville, Sarnafil Roofing, Soprema Canada, Stevens Roofing, Tremco and Trufast
Building Owners	Canada Post Corporation, Department of National Defence, Public Works and Government Services Canada.
Industry Associations	Canadian Roofing Contractors' Association, Canadian Sheet Steel Building Institute, National Roofing Contractors' Association and Roof Consultants Institute.

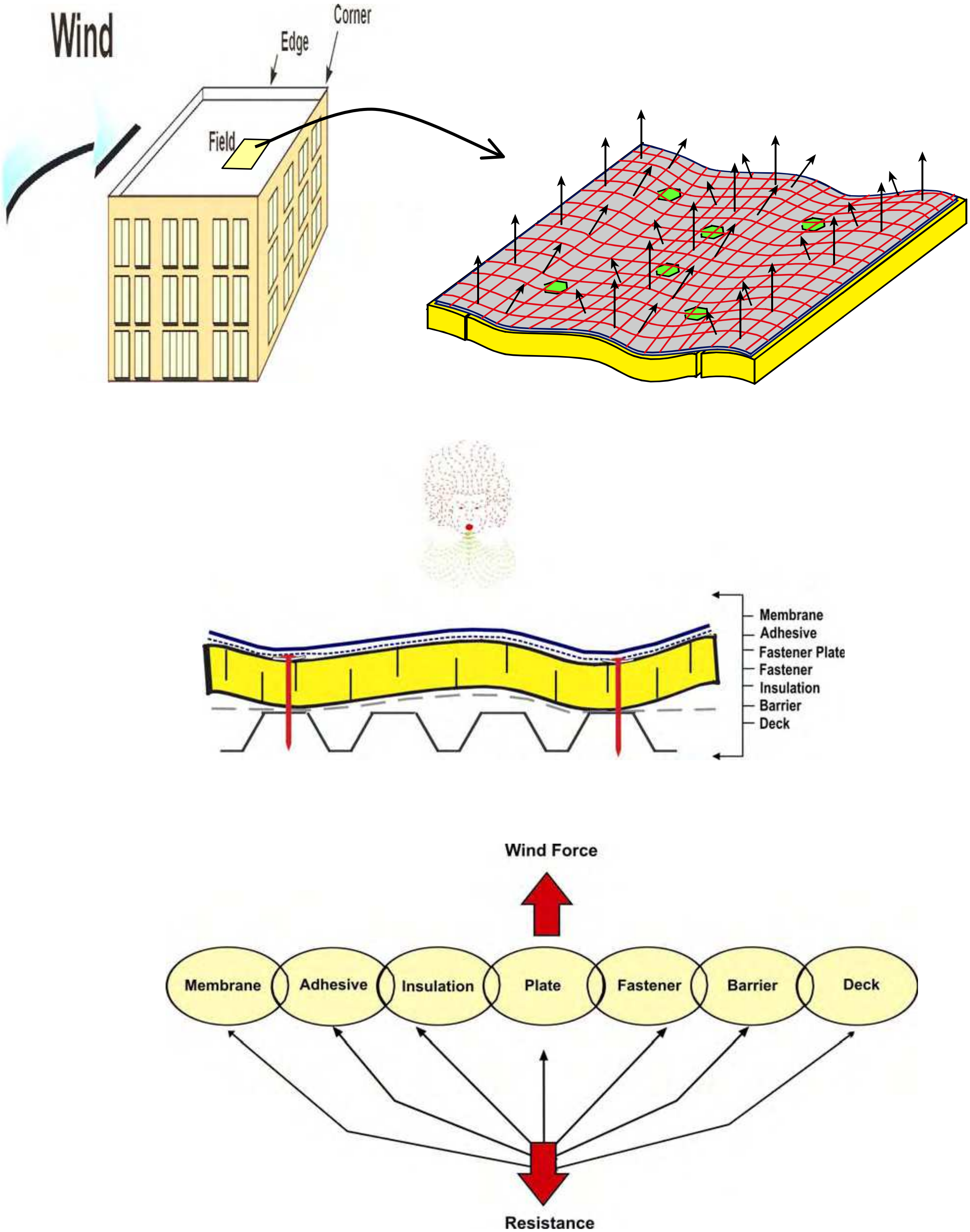

Figure 1. Wind Uplift Resistance of FBA

Figure 2. FBA on the Dynamic Roofing Facility

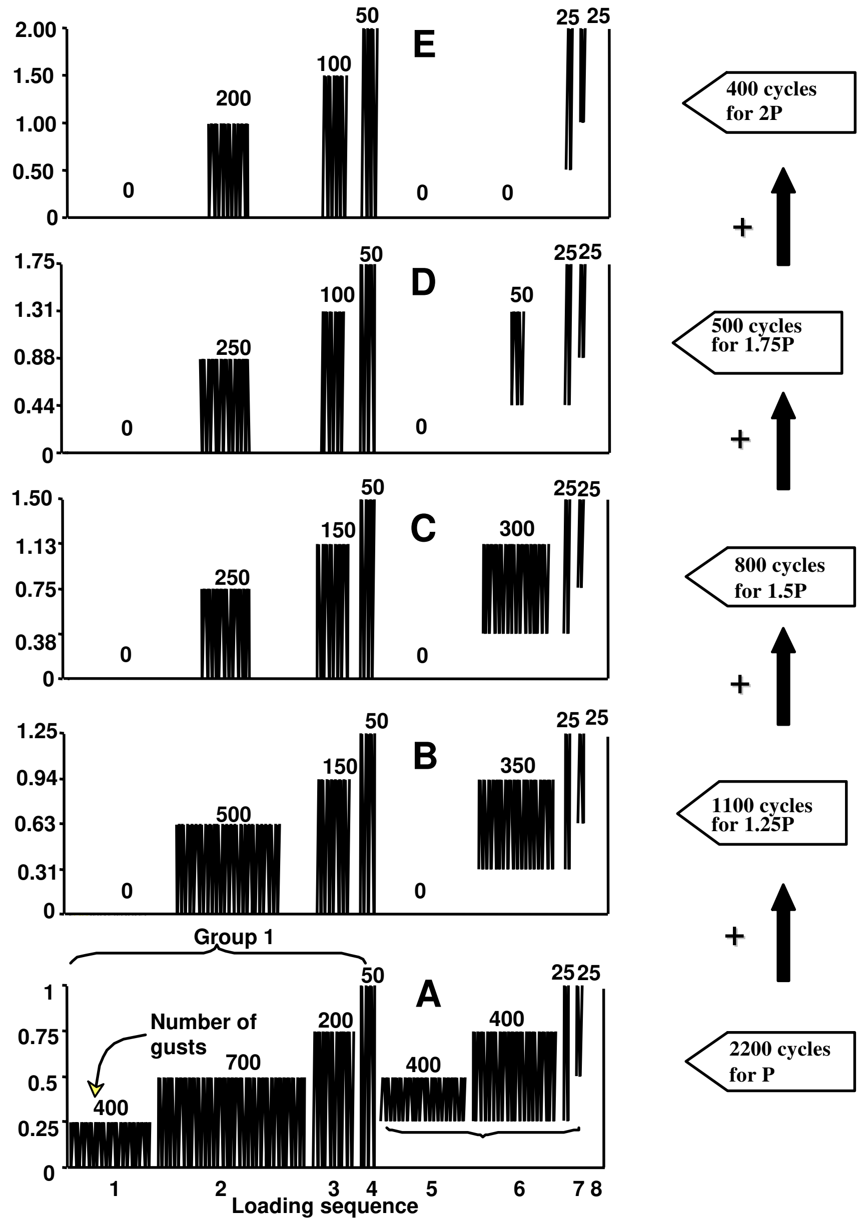

Figure 3. SIGDERS Dynamic Load Cycle

Table 1. Mock-ups Details and Nomenclature

Assembly	**Components**
Assembly **Aref**	Steel Deck – 22- gauge metal Insulation boards – One Layer of 50 mm (2") thick Insulation Fastener Plate - Hexagonal metal plate - 73 mm (2 ⅞ ") diameter Fastener Density – One fastener per 0.17 m^2 (1.8 ft^2) Type # 15 Fastener - 127 mm (5") long Adhesive - 3.79 L / 6.5 Sq. m (1 gal / 70 Sq. ft) Thermoplastic Olefin membrane (TPO) - 45 mil thickness
Assembly 1: A1	Similar to the Aref with the addition of barrier. ***A1 comprises of 12.5 mm (½") support board and a 6 mil Polyethylene Sheet as barrier***
Assembly 2: A2	Similar to the Aref with an additional layer of insulation. ***A2 comprises of two layers of 50 mm (2") thick staggered arrangement of insulation boards with an overall thickness of 100 mm (4")***
Assembly 3 : A3	Similar to Assembly 2 with the addition of barrier ***A 3 comprises of a support board and barrier with two layers of 50 mm (2") thick staggered arrangement of insulation boards***
Assembly 4: A4	Similar to the Assembly 1 with the reduction in fastener density. ***A4 has a fastener density of one fastener per 0.24 m^2 (2.6 ft^2)***
Assembly 5: A5	Similar to the Assembly 1 with the reduction in fastener density ***A5 has a fastener density of one fastener per 0.5 m^2 (5.3 ft^2)***

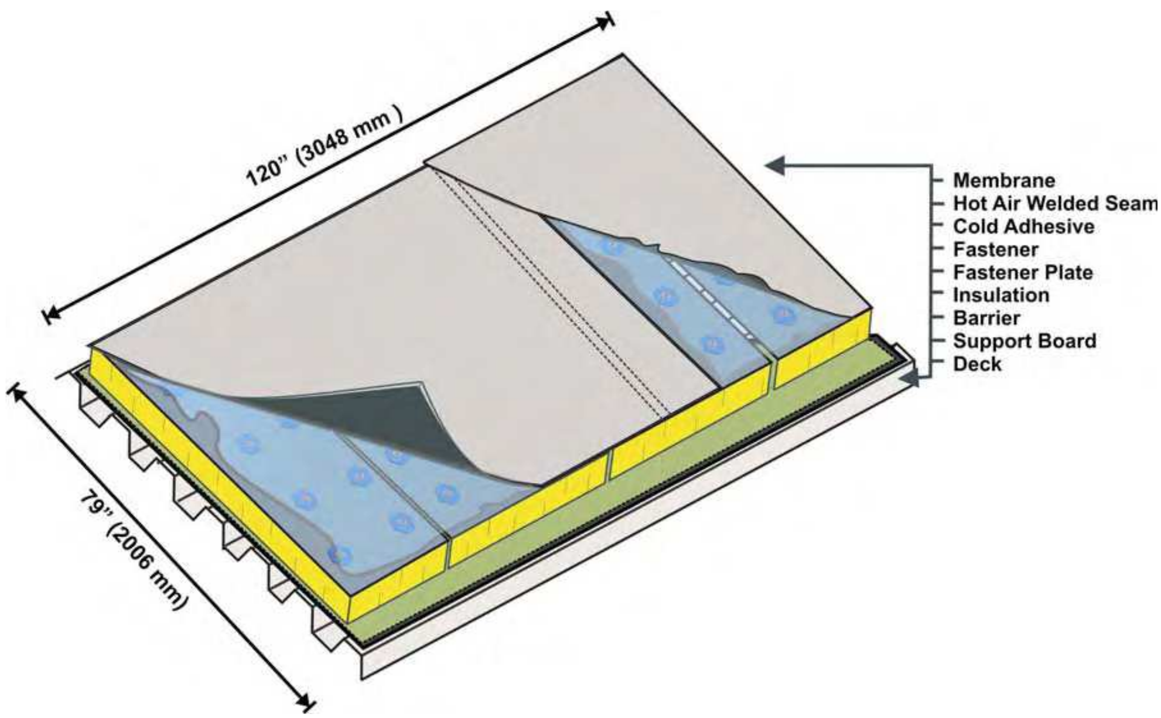

Figure 4. Typical Layout of FBA with Barrier

Figure 5. Mock up Construction Process of FBA with Barrier

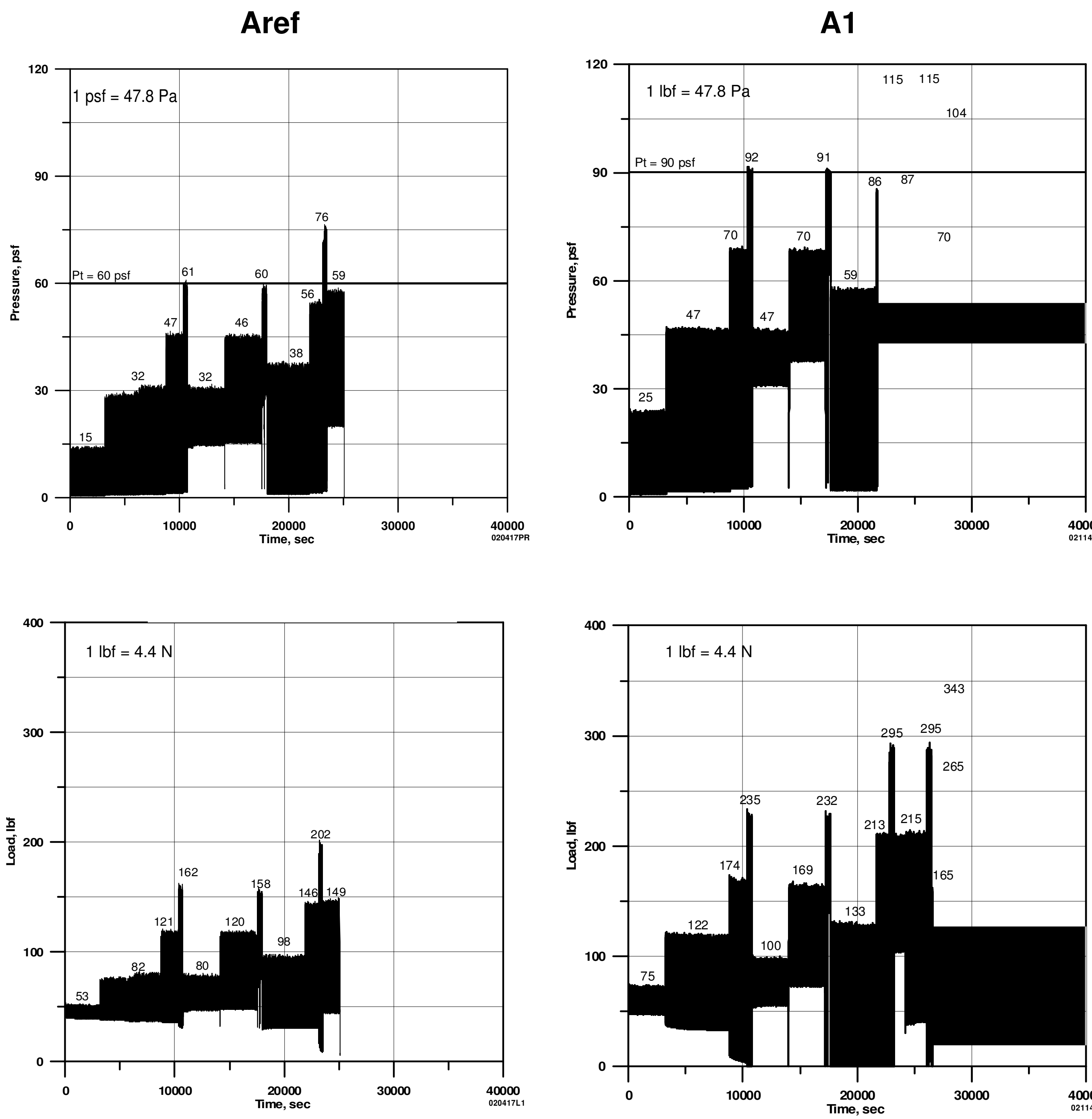

Figure 6. Comparison of the Response Plots of FBA with (A1) and without Barrier (Aref)

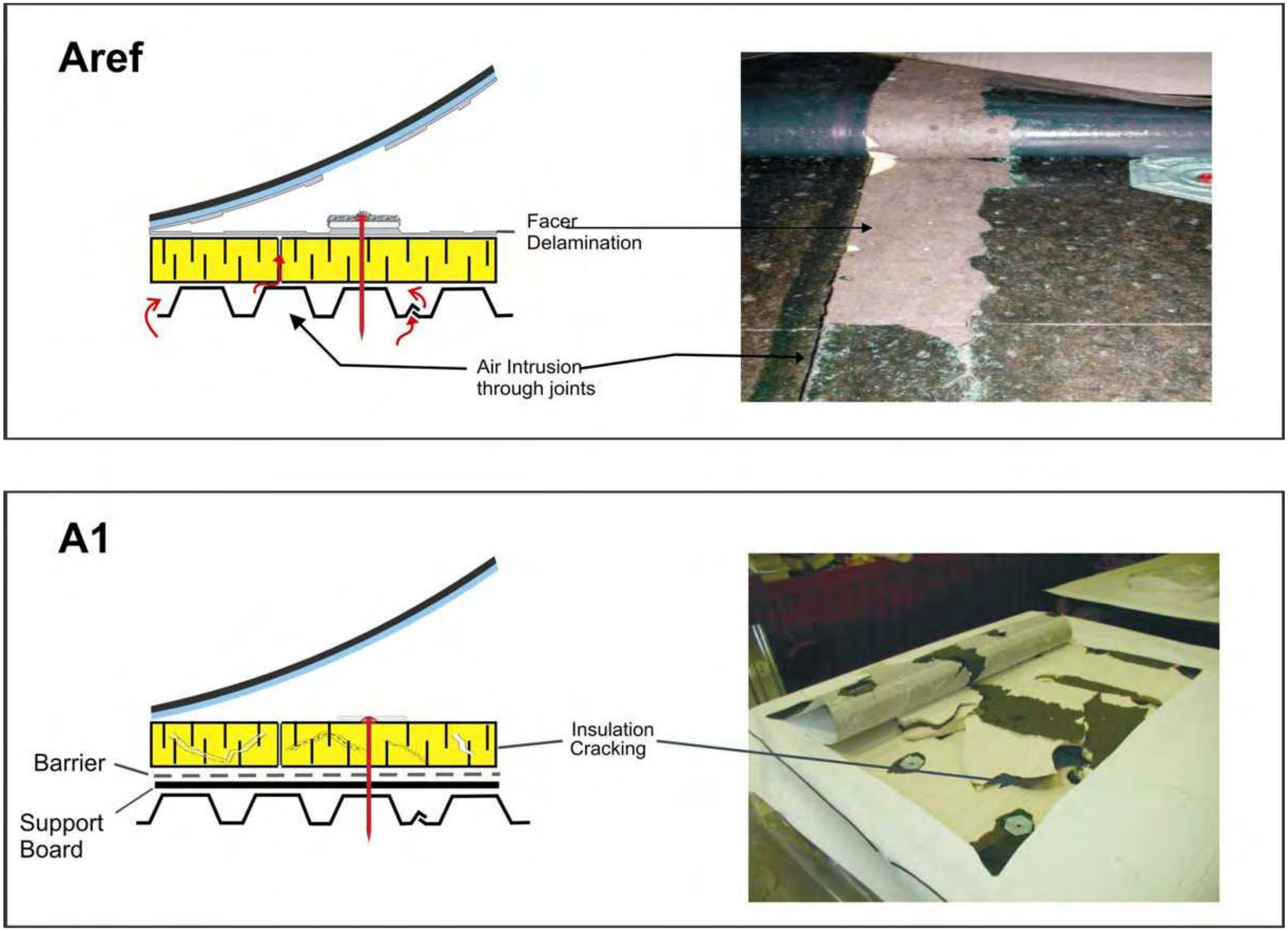

Figure 7. Comparison of the Failure modes of FBA with Barrier (A1) and without Barrier (Aref)

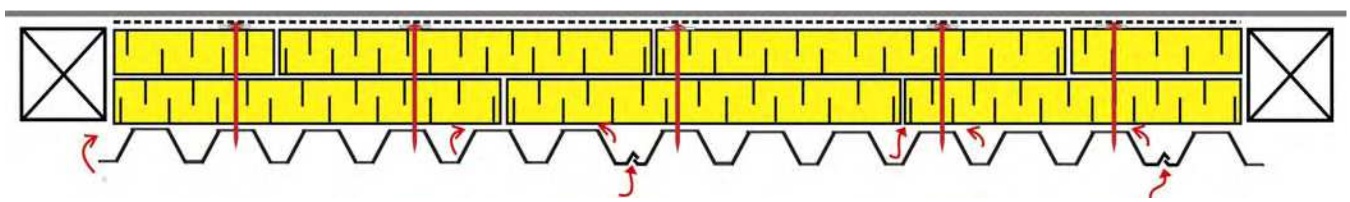

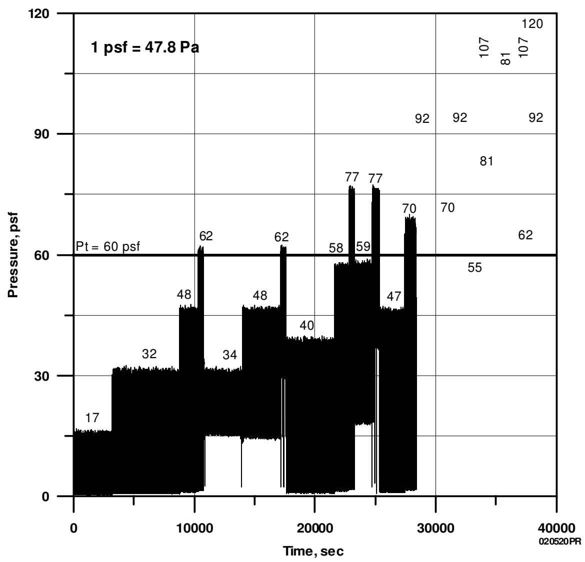

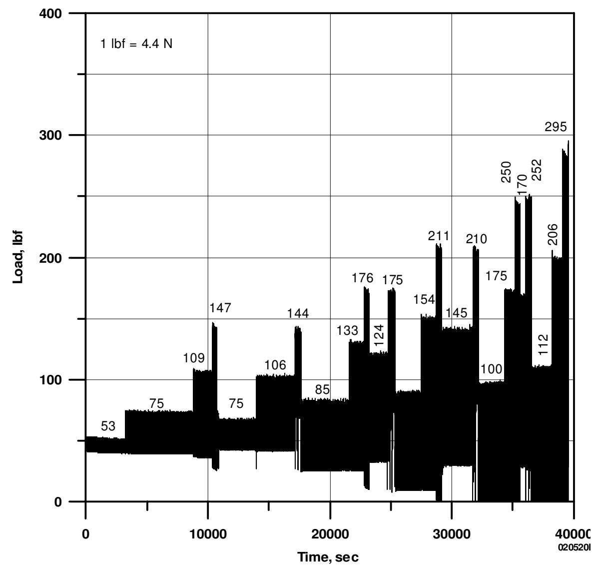

Figure 8. Response of A2 with Staggered Insulation Arrangement – Pressure & Load

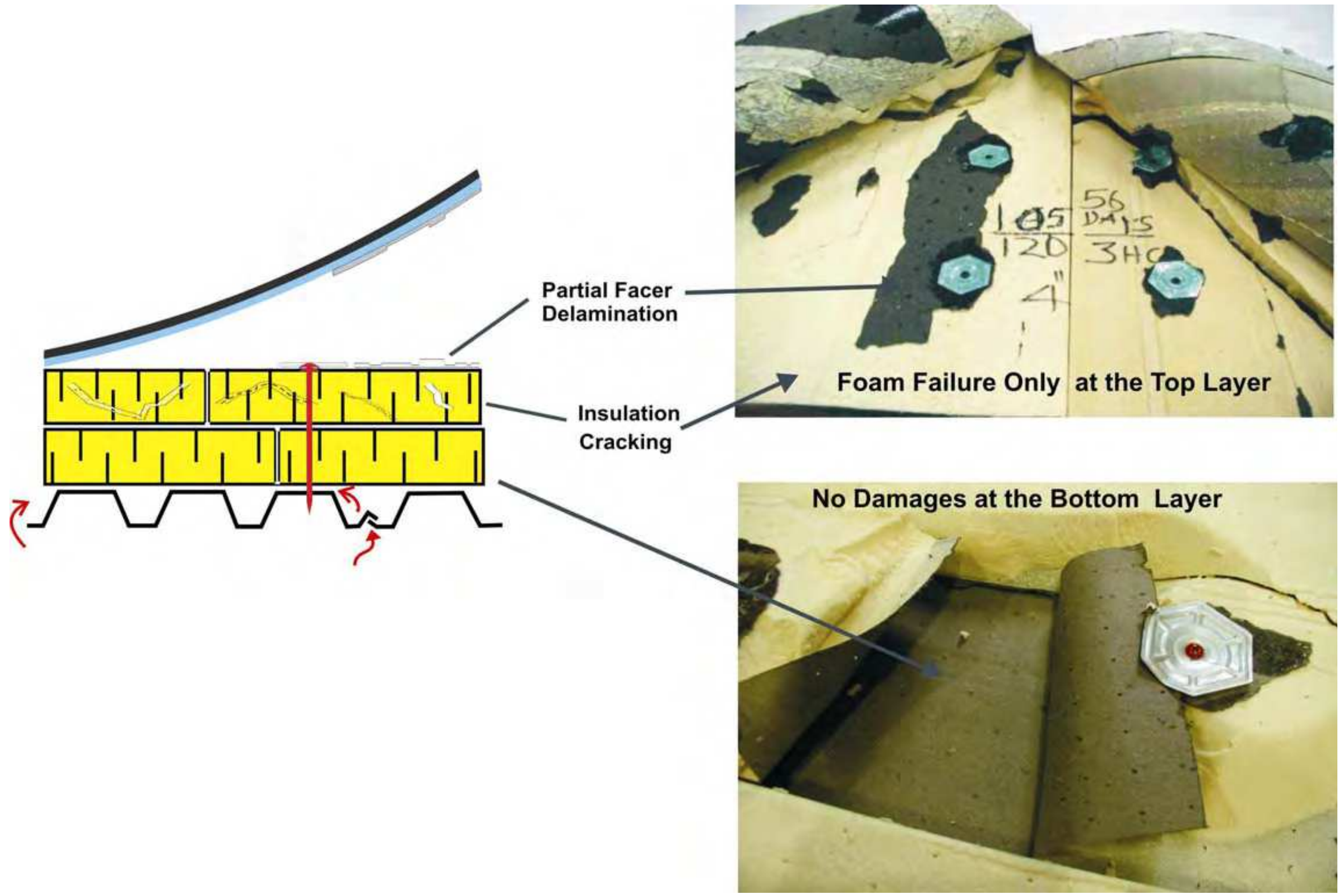

Figure 9. Failure Mode of A2 with Staggered Insulation Arrangement without Barrier

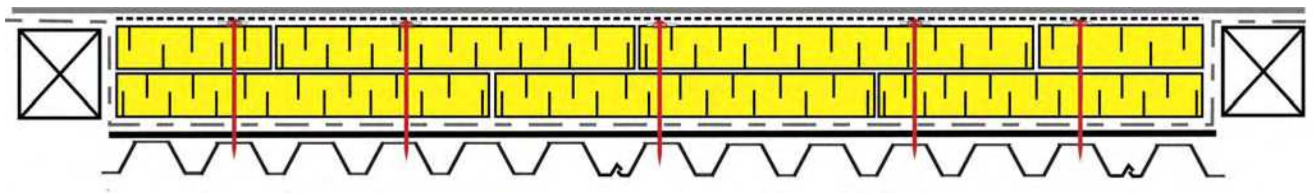

Figure 10(a). Cross Sectional View of A3 - Staggered Insulation Arrangement with Barrier

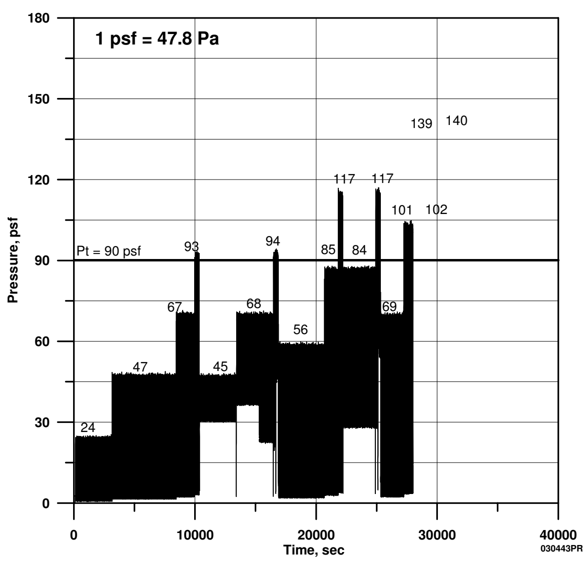

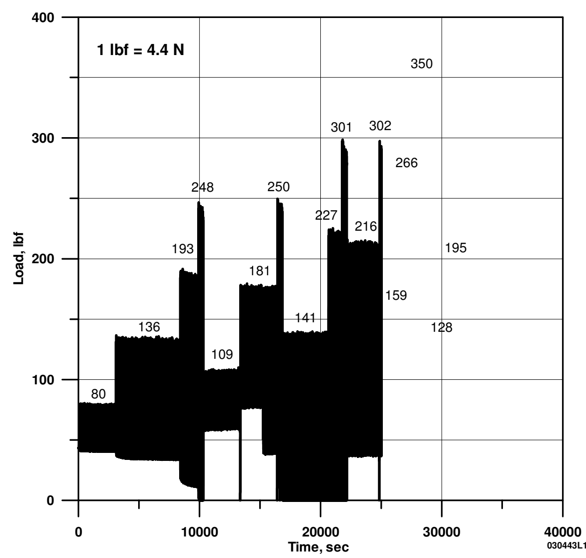

Figure 10(b). A3 Pressure and Load Response

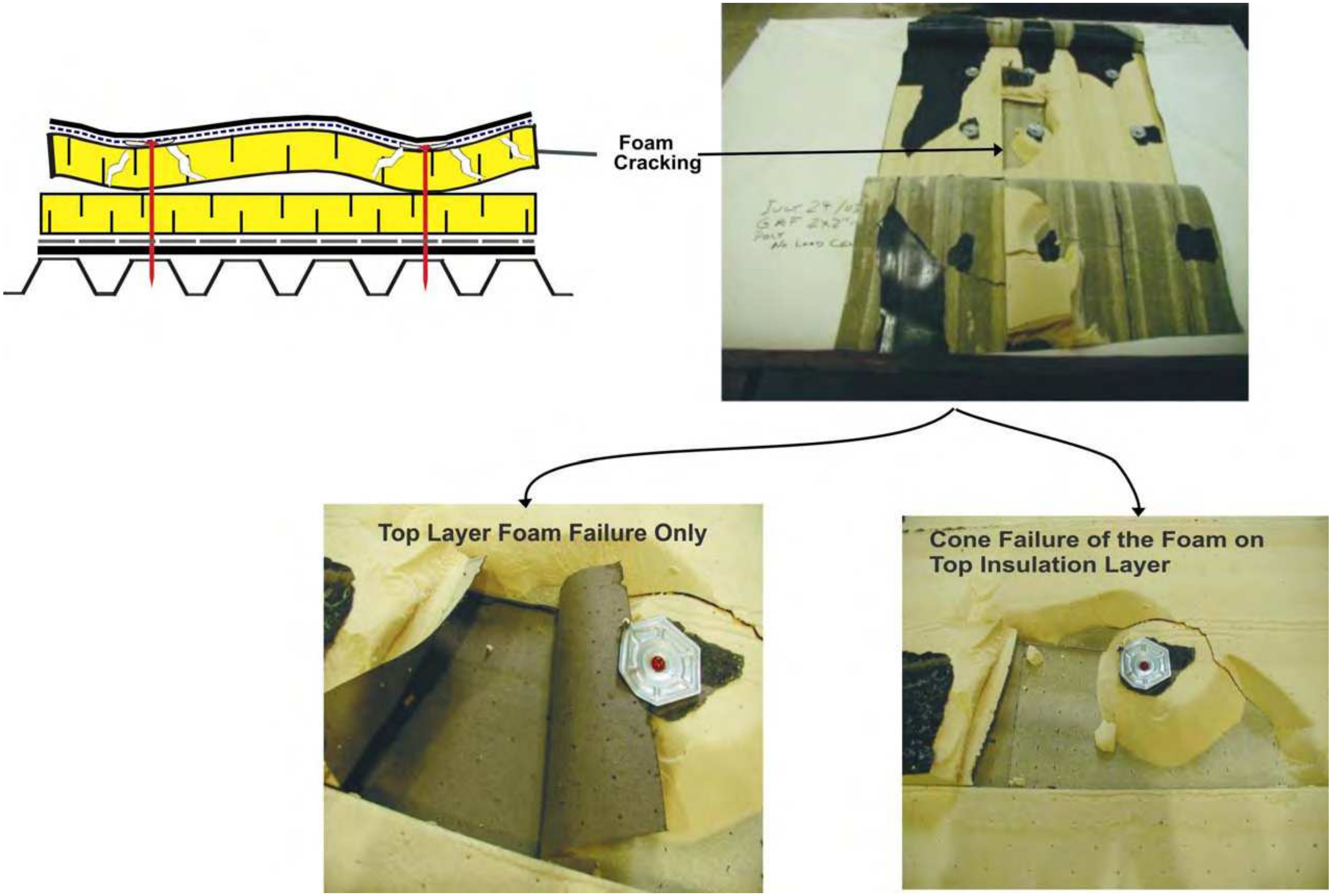

Figure 11. Failure Mode of the A3

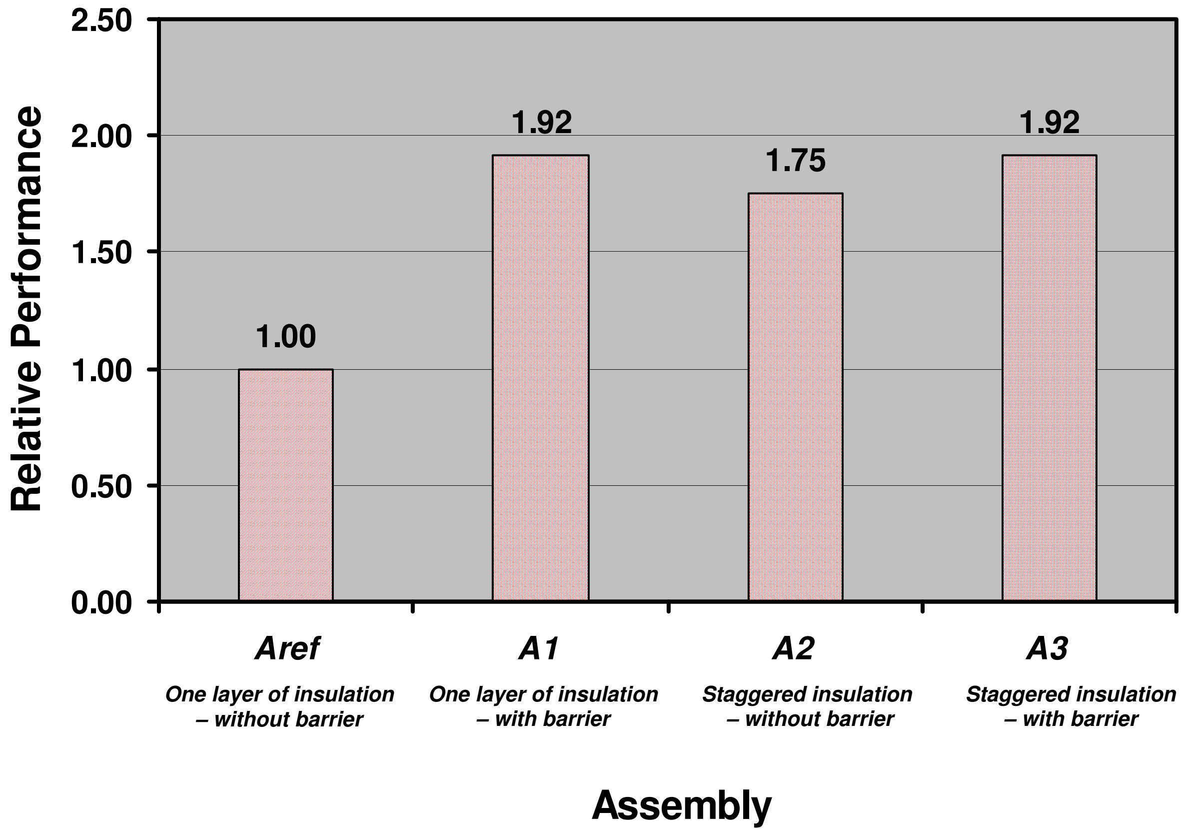

Figure 12. Comparison of the Relative Wind Uplift Performance of FBAs

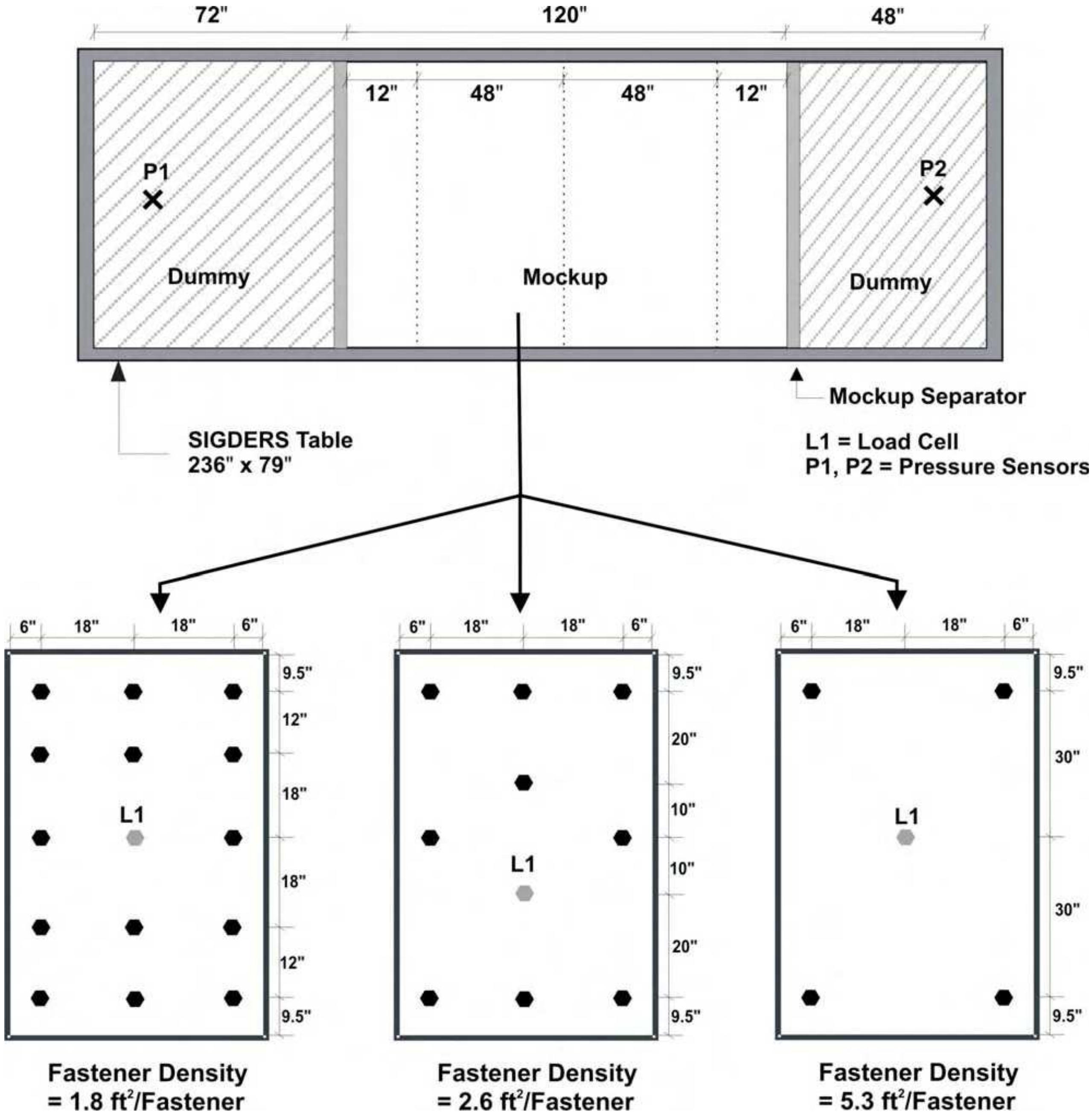

Figure 13. Fastener Density Variations

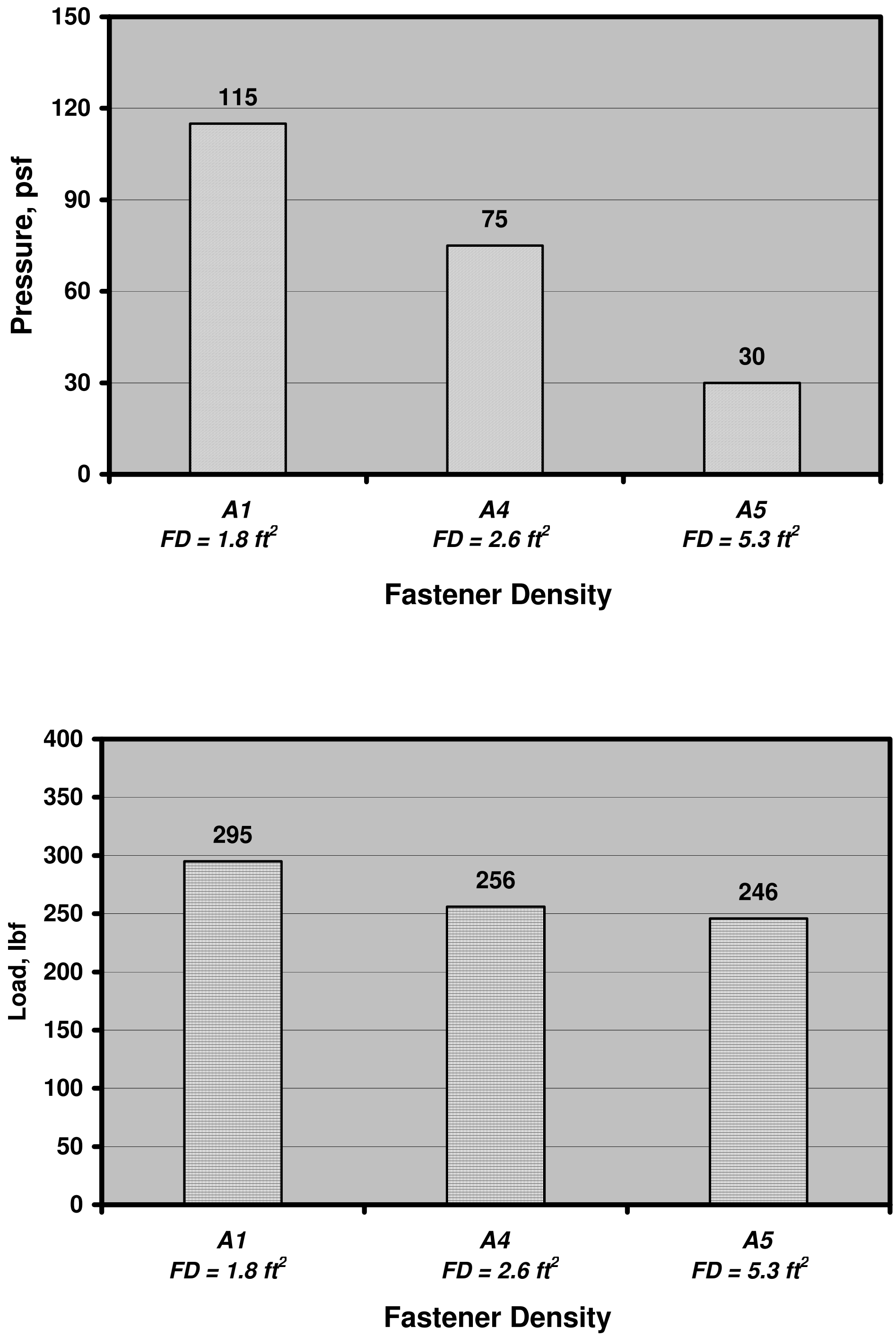

Figure 14. Effect of Fastener Density on the Wind Uplift Rating of FBA with Barrier

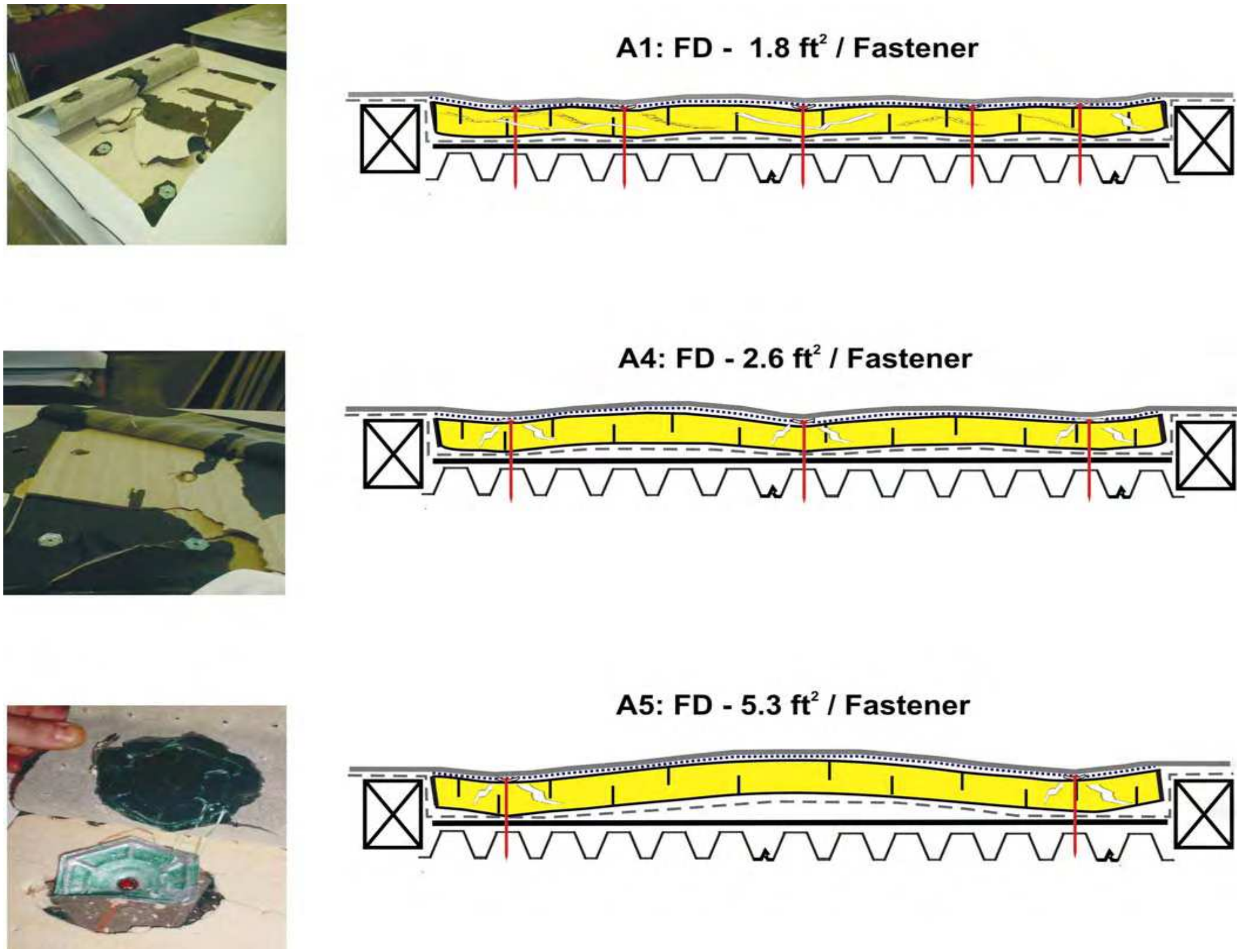

Figure 15. Deformation of the FBAs with Different Fastener Densities